



Seismic Performance Evaluation of Asymmetric Reinforced Concrete Tunnel Form Buildings



Seyed Bahram Beheshti Aval ^{a,*}, Mohammad Javad Asayesh ^b

^a Civil Engineering Faculty, K. N. Toosi University of Technology, Iran

^b Engineering Faculty, University of Science and Culture, Iran

ARTICLE INFO

Article history:

Received 4 December 2016

Received in revised form 21 March 2017

Accepted 21 March 2017

Available online 23 March 2017

Keywords:

Reinforced concrete tunnel form structures

Response modification factor

Asymmetric plan

Incremental dynamic analysis

Performance based earthquake engineering

ABSTRACT

Despite the excellent seismic resistance characteristics of reinforced concrete tunnel form (RCTF) buildings, their predominant torsional vibration modes, especially those related to asymmetric RCTF constructions, make them vulnerable to strong seismic ground motions. For this reason, design guidelines prohibit the construction of multi-story RCTF buildings with asymmetric plans. This lack of relevant code provisions in turn, forces the engineer to apply design methods relevant to typical reinforced concrete (RC) buildings despite the well-known differences in the seismic performance when compared to RCTF buildings. This issue becomes more challenging when one is interested in asymmetric RCTF buildings whose past seismic performance is generally unknown. The present study investigates the seismic performance of two-, five-, and fifteen-story asymmetric RCTF buildings with two distinct plans. A number of parameters such as the percentage of walls at each story level and the in-plan eccentricity, on the lateral capacity of the building subjected to strong ground motions are highlighted. The effect of coupling beams (spandrels) on performance of RCTF constructions is also examined. It is concluded that they do not generally contribute in strength and ductility of low height constructions and in taller ones; due to inducing more demands, these low strength shear-failure-type members fail prematurely. However, if these elements are designed based on building code requirements and implemented with adequate shear reinforcements, they may be used as the structural fuses for dissipating seismic energy. The multilevel performance-based response modification factor (R-factor) is considered in order to capture the seismic performance of the RCTF structures. Relevant demand/supply R-factors are determined for this particular case study involving all the effective parameters such as ductility, over-strength, redundancy, seismic hazard level, and performance level. As a general conclusion, the results of the research show an excellent seismic performance of this type of structures in spite of their inherent irregularities. The high lateral stiffness and strength of the RCTF building compensates for the relatively low torsional stiffness with respect to lateral stiffness; as a result of which, the building exhibits superior seismic performance in high seismic hazard regions.

© 2017 Institution of Structural Engineers. Published by Elsevier Ltd. All rights reserved.

1. Introduction

A reinforced concrete tunnel form (RCTF) building is a modern method of construction that is becoming increasingly popular around the world. The T-shaped formworks allow the builders to cast walls and slabs in one operation during the daily cycle (Fig. 1), improving the construction speed, quality, economy, and accuracy of the in-situ construction [1]. Basically, a RCTF structure is a kind of slab-shear wall system and belongs to the semi-industrial construction method. Due to limited research on their structural behavior under extreme loading, such as strong earthquake loading, the codes do not consider specific

design guidelines for these systems. Thus, despite the distinct seismic behavior compared with other similar constructions, and due to the lack of specific provisions of this type of construction in design codes, their general designs are generally performed based on the provisions of typical reinforced concrete (RC) bearing walls. Three distinct differences between this innovative system and common RC bearing wall system may be recognized as:

- i. Regarding possibility of removing T-shape forms after casting in-situ-concrete and then sufficient hardening, the structural walls cannot be performed on the outer sides of construction.
- ii. Due to pouring concrete in walls and slabs for each story at one stage, the full conjunction between wall and slab is (full continuity) established.
- iii. With reference to several guidelines, minimum wall percentage is applied.

* Corresponding author at: K. N. Toosi University of Technology, Valiasr Street, Tehran, P.O. Box 1996715433, Iran.

E-mail address: beheshti@kntu.ac.ir (S.B. Beheshti Aval).

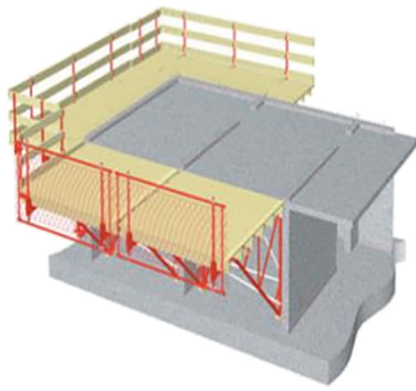


Fig. 1. RCTF construction in Pardis site near Tehran, Iran's capital city.

In recent years, not many publications have focused on the analysis of RCTF buildings subjected to seismic excitation. Balkaya and Kalkan [2] compared the non-linear response of two- and five-story RCTF buildings with similar plans. The results showed that the structural behavior of the three dimensional (3D) model is more accurate than that of the two dimensional (2D) model. Moreover, the total lateral resistance capacities of the 3D models were increased compared to their 2D counterparts. In further research, Kalkan and Yuksel [3] studied the effect of vertical reinforcement ratio and boundary reinforcement on performance enhancement of an H-shaped tunnel-form building under seismic action. The results showed clear differences between the capacity curves in the inelastic region for the same roof drifts while the longitudinal reinforcing percentage increased. These studies confirmed the different behavior patterns between the RCTF and other common RC systems.

Regarding the importance of fundamental natural period and response modification factor (R-factor) in estimation of seismic base shear of structures in seismic design code, the researchers have dedicated their focus on estimating these two major seismic parameters for the new structural system. Among them, Goel and Chopra [4] compared the fundamental periods of vibration of buildings in California region with the formula provided in the design codes of NEHRP-94 [5], SEAOC-96 [6], and UBC-97 [7]. They concluded that the code-based formula for the estimation of the fundamental period of vibration was not sufficiently accurate for RC shear wall buildings. Lee et al. [8] focused on evaluating the accuracy of code formulas (KBC 1988 [9], UBC 1997 [6], NBCC 1995 [10], BSIJ 1994 [11]) for estimating the fundamental period of RC buildings with shear-wall dominant systems. For this purpose, full-scale measurements were performed on a fifty-story RC apartment building. The results were subsequently compared with those obtained by code formulas and by full dynamic analysis. It was deduced that none of examined code formulas were able to sufficiently estimate the fundamental periods of the buildings and therefore they an updated formulation was proposed for the estimation of the fundamental period of such buildings. Balkaya and Kalkan [12] examined eighty RCTF buildings with different plans and elevations, and demonstrated that the use of available empirical relations as suggested by the design codes to estimate the fundamental period of vibration of RCTF systems may lead to inaccurate results. Subsequently, they proposed an equation for the estimation of the fundamental period of the RCTF constructions with a restriction on the maximum height. Given the complexity and limitation of their originally proposed equation, they updated their original formula by studying twenty RCTF constructions in another publication

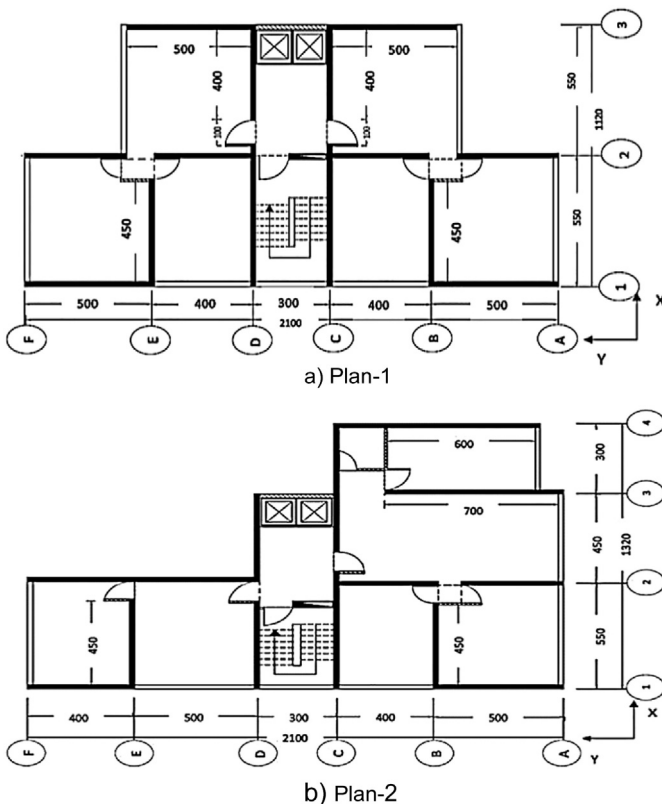


Fig. 2. The Plan of case study RCTF buildings.

Table 1 Geometrical specifications of the case study plans.

	Length (m)	Width (m)	Area (m ²)	Wall percentage ^a	
				(X-direction)	(Y-direction)
Plan-1	11	21	187	3.10	3.85
Plan-2	13	21	193.5	3.10	4.24

^a The ratio of wall's cross-sectional area to total floor area in X or Y direction.

Table 2 Thickness of shear walls in the 15-story building.

	Story	X-direction			Y-direction			
		1	2	3	B	C	D	E
Thickness of shear walls (cm)	1 to 7	30	35	30	30	35	35	30
	8	30	30	30	30	30	30	30
	9	25	25	25	25	25	25	25
	10 to 15	20	20	20	20	20	20	20

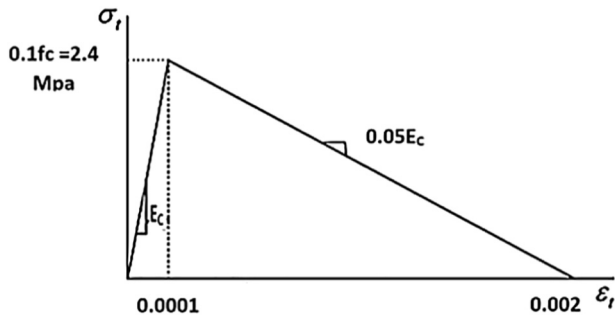


Fig. 3. Tensile behavior of concrete.

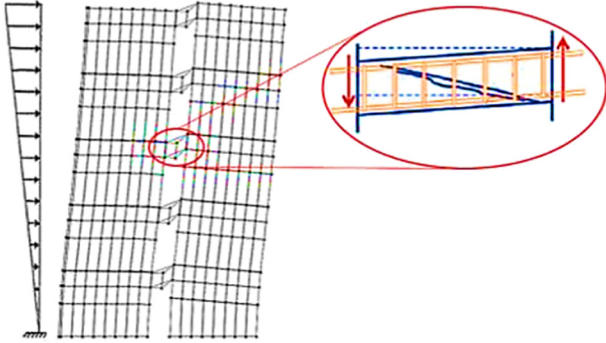


Fig. 4. Shear failure of the spandrels, modeled by the infill panel elements.

[13]. A developed database consisting of ten different plans with different heights (from 5 to 25 stories) by Tavafoghi and Eshghi [14] showed that the formulas according to ASCE/SEI 7-05 [15] are simpler and more accurate than the suggested formulas based on the other references. In a recent study by Eshghi and Tavafoghi [16], the failure mechanisms of two three-story 1/5-scale tunnel form buildings were captured and compared to the finite element model subjected to quasi-static cyclic lateral loading. The fundamental period of cracked structures was also estimated and the non-ductile failure mechanisms of specimens in the shear walls attributed to sudden rebar rupture were also reported.

The second important parameter in the seismic design of buildings is the response modification factor (R-factor). The suitable R-factor for RCTF construction are very rare in the literature. Balkaya and Kalkan [17] proposed the values of 5 and 4 for the R-factor of a two- and five-

story building, respectively. Tavafoghi and Eshghi [18] employed the ATC-63 methodology to evaluate the R-factor for RCTF constructions with five practical plans and different heights from 15 to 45 m. They concluded that except for the boundary zone check, the R-value of 4 is a reliable quantity for these type of structures when the design requirements of ACI 318-05 (ACI, 2005) [19] and ASCE/SEI 7-05 [15] for a bearing wall system are fully satisfied. They claimed that more research is required with an increased number of building types (in terms of plans and elevation) in order to obtain a more reliable prototype value for the R-factor. Due to developing these factors based on engineering judgment and the lack of observation of the seismic performance of structures subjected to past earthquakes, the R-factor has not yet been incorporated into the seismic design codes for RCTF buildings. To overcome this challenging issue, structural engineers design RCTF buildings considering R-factors applicable to RC bearing wall structures.

In this article, a multi-level definition of the R-factor is given and its derivation is related to the seismic intensity, and the accepted damage level. In contrast to all previously mentioned studies, the demand/capacity R-factor is determined in a more accurate way by involving several effective parameters of the structural system such as ductility, overstrength, redundancy, seismic hazard level, and the target performance level.

Apart from lacking the reliable R-factor, two restricted issues prevent the use of this structural system in urban areas, especially in densely populated districts. One is the limited available indoor parking area at ground floor level due to the need for a minimum percentage of shear walls (shear wall area to floor area ratio should be more than 2%). Another restriction is associated with the design of the architectural plan pertaining to prohibition of using asymmetric configurations. The first issue will not be examined further in this study. The second issue originated from several supplementary guidelines such as Building and Housing Research Center of Iran [20] and Turkish standard [21]. This concern comes from the inability of RCTF constructions to withstand lateral seismic loads pertaining to their low torsional resistance against twist movements. As a matter of fact, owing to practical considerations and the necessity for removing forms after casting concrete, it is not possible to use structural walls in the exterior sides of these buildings and so as a result, torsional stiffness of these constructions is far less than their lateral stiffness. For this reason, such constructions may produce poor performance against torsional movements during strong earthquakes. Therefore, application of irregular RCTF systems in high seismicity area is questionable [22].

Two main questions are required to be properly addressed prior to deciding on the applicability of RCTF buildings in residential areas. The first one is related to the low torsional stiffness of such structures in

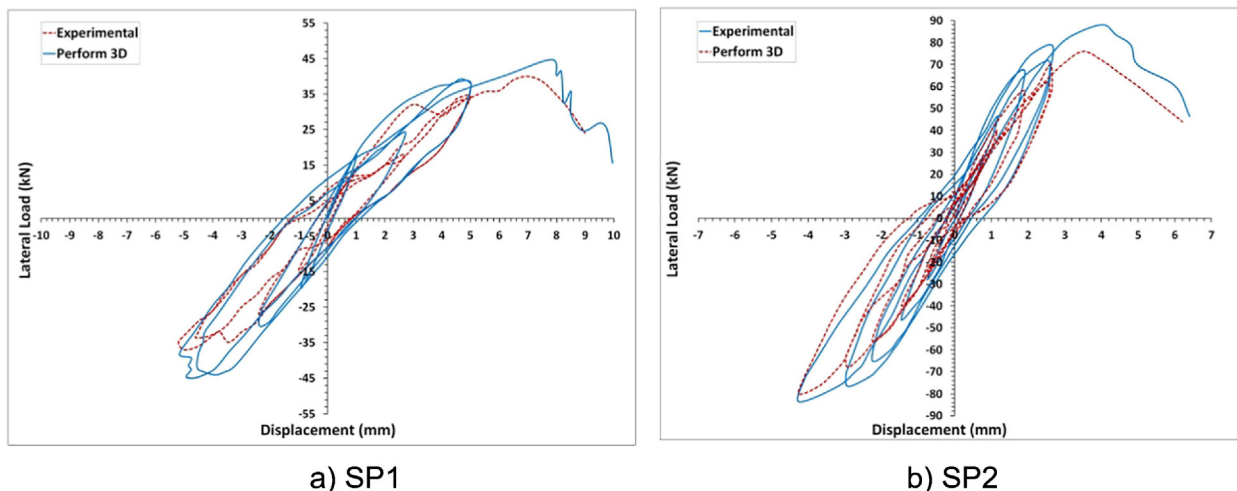


Fig. 5. Comparison of the lateral load-displacement response at roof story level for specimens, SP1 and SP2 of Yuksel and Kalkan and the present modeling [30].

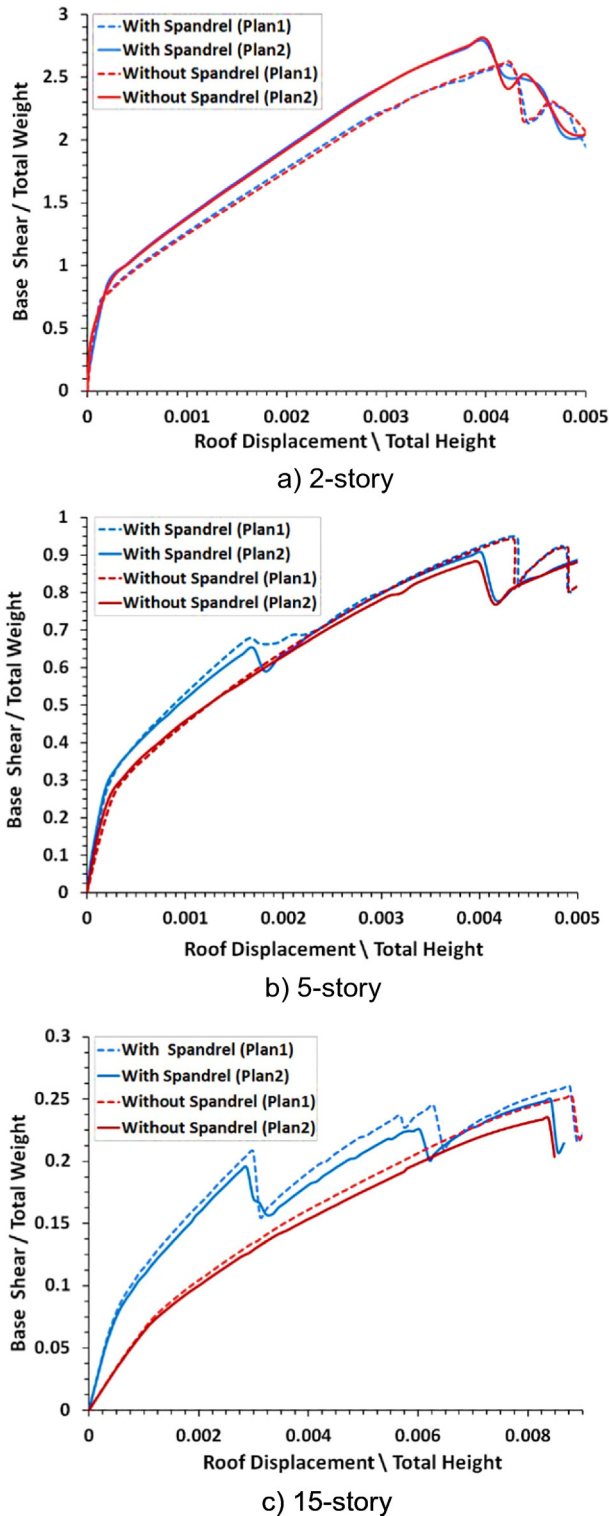


Fig. 6. The base shear-roof displacement curves for case study structures (Plan-1, 2).

respect to the lateral stiffness of the building. In general, the low torsional stiffness is disadvantageous; however, it cannot be examined independently from the lateral stiffness of the building. This point forms a key subject of discussion in this paper. The second question is relevant to the possibility of asymmetric plan of such buildings to satisfy the seismic requirements with adequate torsional strength. Basically, these two questions are not adequately addressed in the literature so far and certainly not in a degree that will allow one to reach solid conclusions on the elements discussed above. This study aims to fill this gap by

examining the seismic performance of two case studies of irregular RCTF constructions using pushover and Incremental Dynamic Analysis (IDA). The analyses have been performed considering two directional excitations. Despite the lack of the response modification factor for this type of building in available research reports, the multilevel definition of behavior factor as the important seismic design parameter is evaluated.

2. Design assumptions

The present study focuses on two-, five-, and fifteen-story buildings with Plan-1 and Plan-2, shown in Fig. 2(a) and Fig. 2(b), respectively and located in Tehran city. The proposed buildings are assumed as residential buildings located on soil type B ($375 \text{ m/s} \leq V_s \leq 750 \text{ m/s}$) in high seismicity areas based on seismic code ISIRI-2800. The ratio of the wall area to the floor area in two horizontal directions, i.e. defined hereafter as the wall percentage, is summarized in Table 1.

The eccentricity in the Y-direction (e_x) and the eccentricity in X-direction (e_y) for Plan-1 and Plan-2 are $e_x = 7.3\%$, 12.3% and $e_y = 0$, 5.2% , respectively. The design of buildings is based on the following standards: (i) Gravitational loading: Iranian National Building Codes, (INBC, Part 6) [23]; (ii) Seismic Loading: Iranian Code of Practice for Seismic Resistant Design of Buildings (2800 Standard) [24]; and (iii) Design of reinforced concrete structures: American Concrete Institute (ACI 318) [19].

The analyzed buildings belong to horizontally irregularly building plans as per seismic code provisions. The compressive strength of concrete and the tensile yield strength of the steel reinforcement are assumed equal to 24 and 400 MPa, respectively. The thickness of the various walls of the two- and five-story buildings is equal to 20 cm while for the fifteen-story building the wall thicknesses are summarized in Table 2. The thickness of the floor slabs as well as the heights of all the stories are taken equal to 15 cm and 300 cm, respectively. Imposed dead loads of floors and roof are 1.1 kN/m^2 and 1.5 kN/m^2 , respectively. Live loads on floors, roof, and staircases are taken equal to 2.0 kN/m^2 , 1.5 and 3.5 kN/m^2 , respectively.

3. Analytical modeling

The software Perform-3D [25] is used for the seismic analysis because of its high capability to model RC wall members and to evaluate accordingly their seismic performance. The software has considerable capabilities in: (i) modeling the behavior of the various materials; (ii) accounting for the axial-bending interaction behavior of the wall members by using fiber elements; and (iii) allocating the shear behavior of the wall sections in the form of generalized stress-strain curves. The Mander [26,27] and Esmaily-Xiao [28] models are used for simulating the behavior of concrete and steel reinforcing bars. The importance of cracking behavior of concrete in these constructions is modeled in the present study by assuming the relevant values given in Fig. 3.

Considering the large number of shear walls in the RCTF buildings, the walls and hence the coupling beams (spandrels) between them are designed as thin members. Placing diagonal reinforcements as per ACI 318 [19] for enhancing the shear resistance of spandrels with low thickness is practically complicated. Thus, these reinforcements are not usually implemented. As a consequence, shear failure modes develop before the formation of any plastic hinges at the spandrel ends. In analytical modeling, these elements need to be considered as members whose behaviors are predominated by the shear failure mechanism (Fig. 4). So, the infill panel elements with shear stiffness are allocated to model spandrels [29]. The diaphragms and shear walls are modeled with elastic and inelastic shell element, respectively. The walls on the first story are connected to the base in the rotationally-fixed manner. It should also be mentioned that soil-structure interaction effects are not considered in analytical modeling.

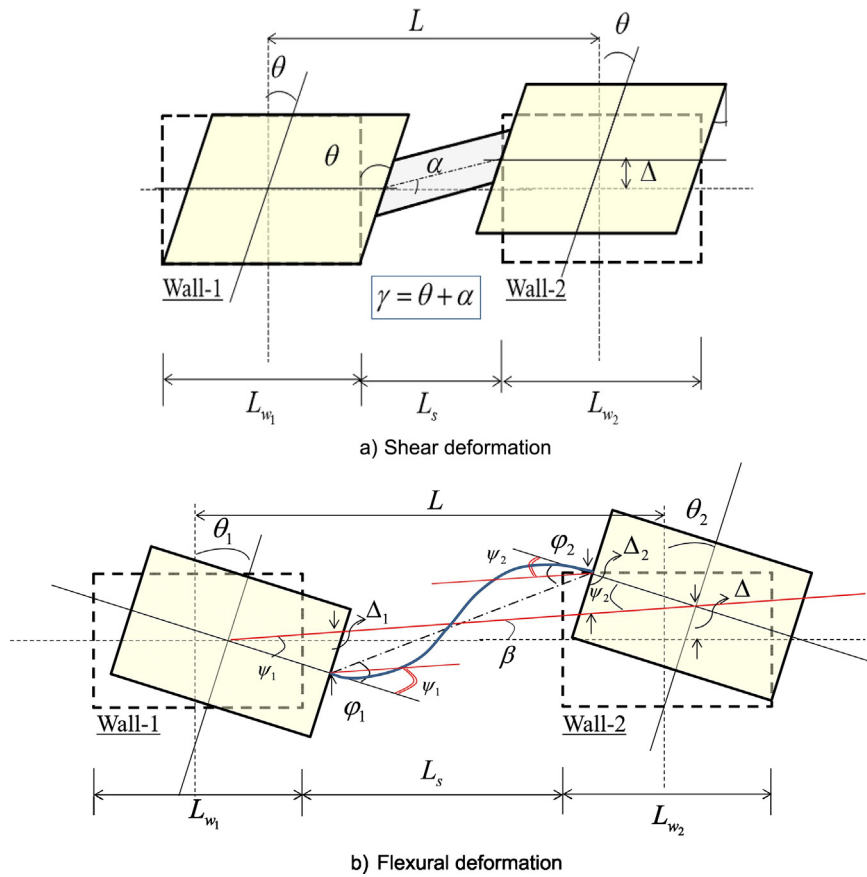


Fig. 7. Distortion demand on the spandrels.

4. Modeling verification

To assess the accuracy of the results obtained from the software Perform 3D, four-story RCTF building tested by Yuksel and Kalkan [30] is modeled using all material properties assumptions mentioned in that paper. The cyclic test results of two specimens SP1 and SP2 are shown in Fig. 5 in which the development of the base shear (vertical axis) is plotted versus the roof displacement (horizontal axis). The finite element results refer to the nonlinear static pushover analysis with a concentrated lateral load at roof level. The resulted hysteresis curves are depicted on the same co-ordinate of Fig. 5. The comparison shows that the predictions of the current model agree reasonably well to the test results for both specimens with a reasonable accuracy.

The slight stiffness and strength differences between the predictions of the two models are attributed to several reasons such as assuming perfect bond for reinforcements, and using coarse mesh and elastic shell element of Perform 3D in comparison with experimental evidences where concrete cracking and reinforcement yielding in slabs may be caused. As can be seen this assumption in Perform 3D has not caused significant error in estimation of the construction strength.

Table 3
Drift rotation values of the roof mass center corresponding to the performance levels.

	Plan	Spandrel (IO)	Spandrel (LS)	Shear wall (IO)	Shear wall (LS)
2-Story	1	0.002100	0.003785	0.003219	0.004300
	2	0.001984	0.003791	0.003181	0.004000
5-Story	1	0.001331	0.001933	0.003073	0.004400
	2	0.001354	0.001964	0.003118	0.003984
15-Story	1	0.002505	0.003118	0.004577	0.008768
	2	0.002429	0.002679	0.004312	0.008503

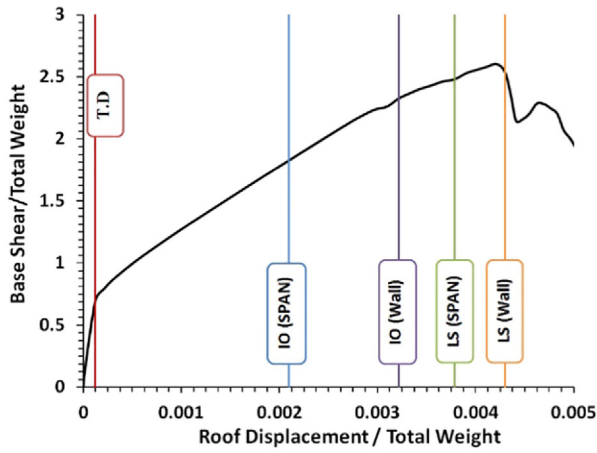
5. Effectiveness of spandrels in overall capacity

To investigate the specific role of the spandrels in strength and ductility of the case study structures, the buildings are analyzed by the classical non-linear static pushover method in two ways: first, the spandrels are included in the model and subsequently, the model is developed in such a way that the spandrels are excluded altogether. In both cases, a triangular load pattern is considered to represent the seismic action in both horizontal directions. A lateral load associated with 100% target displacement is applied along the Y-coordinate (major axis with larger eccentricity), while at the same time a lateral load corresponding to 30% of the target displacement along the X-coordinate (with smaller eccentricity) is considered.

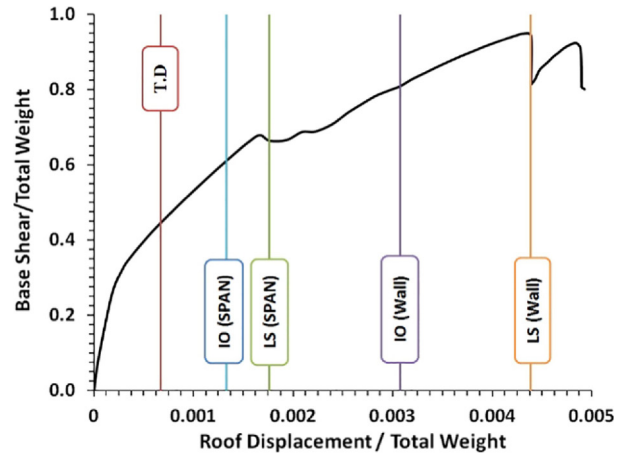
Fig. 6 shows the base shear versus the displacement of the roof mass center of 2-, 5- and 15-story constructions with and without spandrels for both plans in the same coordinate system to assess the impacts of the spandrels on resistance of the constructions. By comparing the diagrams, it may be concluded that the spandrels do not have a significant effect on the ductility and strength of the lower height case study buildings whereas with increasing height their contribution becomes more pronounced. Fig. 7 confirms this observation. The induced shear deformation on spandrel is calculated from the inter-story drift and the

Table 4
Target displacements obtained using ASCE/SEI 41-13 method.

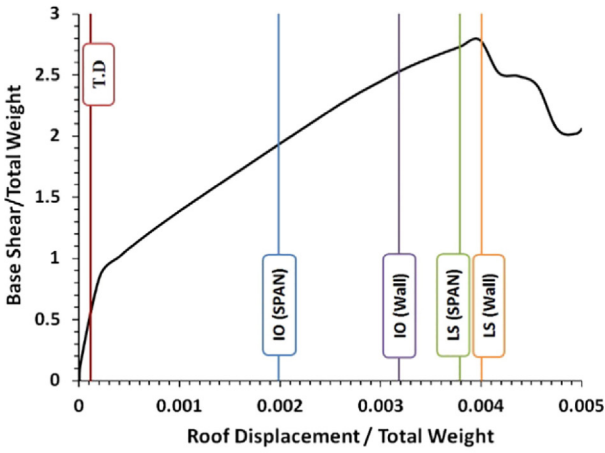
	Plan	Sa	Te	Target displacement (TD)
2-Story	1	0.875	0.05205	0.0001179
	2	0.875	0.05108	0.0001135
5-Story	1	0.875	0.17470	0.0006725
	2	0.875	0.15760	0.0006020
15-Story	1	0.783	0.76080	0.003865
	2	0.783	0.69023	0.003351



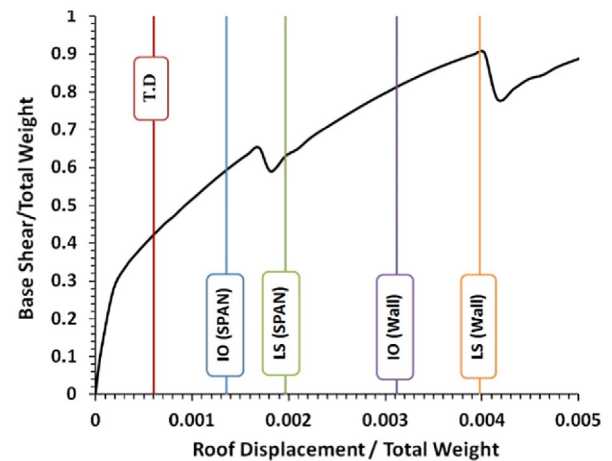
a) Plan-1



a) Plan-1



b) Plan-2



b) Plan-2

Fig. 8. Performance evaluation of the 2-story structure.

Fig. 9. Performance evaluation of the 5-story structure.

associated chord rotation. The chord rotation is acquired from the racking deformation. The shear load is applied to a spandrel through relative shear displacement of the two adjacent walls at its ends. Since the walls are constrained by the in-plan-rigid floors, they deflect laterally by the same amount at the correspondent floor level. As the rotations of the walls are equal to the rate of change of lateral deflection with height, the walls also rotate by the same amount at the same floor level. Thus, the rotations of the two ends of a spandrel should be the same, as illustrated in Fig. 7(a). The shear strain γ can be estimated as:

$$\gamma = \alpha + \theta \tag{1}$$

Where, α is chord rotation and θ is inter-story drift ratio. For lower height constructions, $\alpha = 0$ and hence, racking deformation angle equals inter-story drift ratio. It can be concluded that shear deformation demand and its effect on overall stiffness and ductility of construction is increased for taller building.

Spandrels with aspect ratios greater than four are considered as shallow beams with dominant flexural deformation (compared to the shear deformation). The kinematic deformation of these spandrels is depicted in Fig. 7(b). A simple calculation can point out the induced flexural rotations at the ends. If β is considered as racking deformation angle, one obtains:

$$\beta = \frac{\Delta}{L} \tag{2}$$

The rotation of each wall with respect to the line intersecting their centers is:

$$\psi_i = \theta_i + \beta \quad ; \quad i = 1, 2 \tag{3}$$

Moreover, the deflections of the walls' centers corresponding to this line are equal to:

$$\Delta_i = \frac{L_{W_i}}{2} \cdot \psi_i \quad ; \quad i = 1, 2 \tag{4}$$

Based on the geometry shown in Fig. 7(b), the end-rotations of spandrel are:

$$\varphi_i = \psi_i + \frac{\sum_{j=1}^2 \Delta_j}{L_s} \quad ; \quad i = 1, 2 \tag{5}$$

For a low-rise building with rigid floor and walls with uniform thickness, the relationship between the rotation at the spandrel ends and the inter-story drift ratio reads:

$$\varphi_i = \theta \left(1 + \frac{L_w}{L_s} \right) \tag{6}$$

This equation is equivalent to the one reported by other researchers for plastic hinge rotations of shallow spandrels governed by flexural deformation patterns [31].

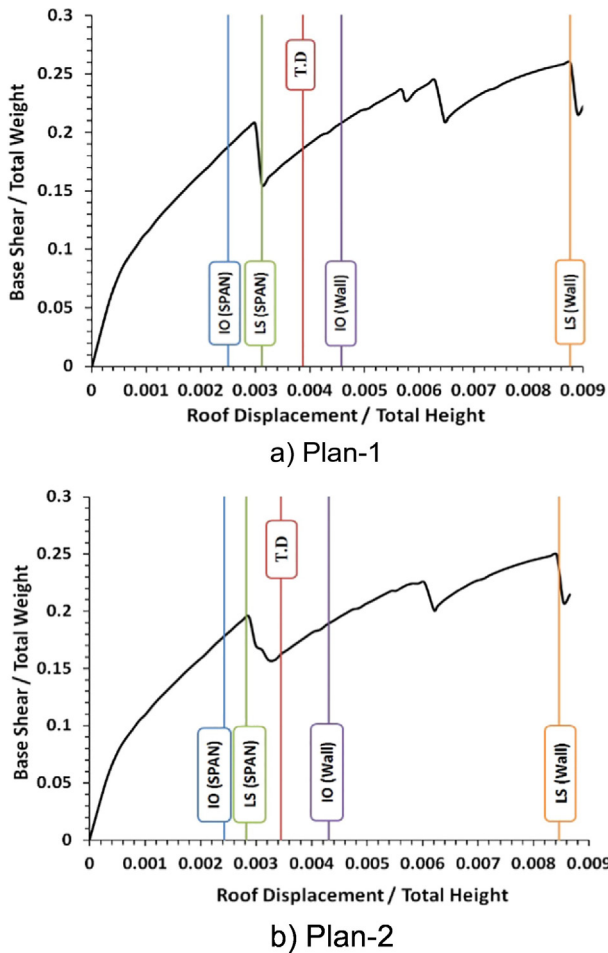


Fig. 10. Performance evaluation of the 15-story structure.

As can be seen by the obtained capacity curves, the spandrels do not have considerable effect on the lateral capacity of 2-story at all, whereas, the drift demand for 5-story is after 0.2%, and for 15-story after 0.65%. Eq. (1) indicates that for low height construction (e.g. 2-story case study construction), due to low chord rotation, the low shear deformation demand is applied and hence, the spandrels would not encounter serious damage, but instead, would contribute in ductility and lateral shear strength of construction. With increasing construction height (e.g., 15-story case study construction), the racking deformation angle of spandrels as per Eq. (2) is increased pertaining to flexural

Table 5 Specifications of selected records for performing time history analyses.

Record	Registration station	M _s	Distance from fault (km)	Component	PGA
Cape Mendocino	89509 Eureka	7.1	44.6	0	0.154
				90	0.178
Cape Mendocino	89486 Fortuna	7.1	23.6	0	0.116
				90	0.114
Northridge	90018 Hollywood	6.7	25.7	90	0.136
				180	0.245
Northridge	24523 Lake Hughes	6.7	32.3	0	0.036
				90	0.063
Northridge	90061 Big Tujunga	6.7	24	0	0.163
				90	0.245
Landers	23559 Barstow	7.4	36.1	0	0.132
				90	0.135
San Fernando	80053 Pasadena	6.6	31.7	0	0.088
				90	0.110

deformation of adjacent walls especially at upper stories. Due to low shear strength of these spandrels, the greater shear deformation demands cause damages in these elements, which can be seen in dropping lateral strength in capacity curves in Fig. 6. However, if these elements are designed and implemented based on design requirement and provided adequate shear reinforcements, the spandrels can play as the structural energy-dissipating fuses, due to more shear distortion demand under seismic loading.

6. The performance levels

After dividing structural members into the primary and the secondary elements, Tables 10–19 and 10-20 of ASCE/SEI 41-13 [32] may be used to collect modeling parameters and acceptance criteria of the members controlled by bending and shear respectively. In order to compare performance levels of different members of a structure, it is necessary to introduce these performance levels to all members of a construction using a single index. Drift ratio of roof mass center can be used as a suitable index for performance level identification. To this end, the roof drift ratio in which the relevant performance level violated at each construction member is recorded in pushover analysis. Table 3 shows drift rotation values of roof mass center corresponding to IO and LS performance levels of the shear walls and the spandrels.

For performance evaluation of the case study constructions, the target displacement of each construction is calculated and compared with the displacement values corresponding to the performance levels obtained from the earlier step. The target displacements are calculated using two different methods; once using the ASCE/SEI 41-13 [32] coefficients method and then using response history analyses [33].

The target displacement δ_t is estimated based on Eq. (7) and its relevant coefficients C_i are evaluated as per definition in ASCE/SEI 41-13 [32]. Table 4 shows the target displacements for different constructions under site-specific spectra at the 10%/50 year probability of exceedance.

$$\delta_t = C_0 C_1 C_2 S_a \frac{T_e^2}{4\pi^2} g \tag{7}$$

In which:

C_i = Coefficients to modify maximum displacement of equivalent elastic Single-Degree-Of-Freedom (SDOF) to actual Multi-Degree-Of-Freedom (MDOF) structures as per ASCE/SEI 41-13 [32].

T_e = Fundamental natural period of MDOF structure.

$S_{a,g}$ = Spectral acceleration at the first natural period and gravitational acceleration, respectively.

Figs. 8-10 attempt to compare the target displacements and the displacement corresponding to each performance level which are drawn as vertical lines on the base shear-roof drift diagrams obtained from non-linear static analysis of each construction. Surveying the figures shows that the 2- and 5-story RCTF buildings are in Immediate Occupancy (IO) performance level. For the 15-story constructions, IO and LS performance levels are violated at spandrels; however, the shear walls are still at the IO performance level. If the spandrels are considered as the secondary elements, it can be concluded that the 15-story constructions similar to 2- and 5-story constructions is at the IO performance level. Therefore, the results show an appropriate seismic performance of the case study RCTF structures in spite of some irregularities in their plans.

To be confident of achieving the performance conditions of the constructions under study, target displacements are determined using non-linear time history analysis, which is more accurate than pushover analysis. Seven couple accelerograms with reverse normal faulting mechanism and magnitude between 6.5 and 7.5 are used. The predominant component of each couple earthquakes is applied in the direction perpendicular to larger eccentricity. The accelerograms are devoted to class B of USGS soil classifications that correspond to soil type II of Iranian 2800 standard. The distance between recording stations and earthquake source is within 23–45 km. Table 5 shows the specifications

Table 6
Target displacement obtained by time history analysis.

Record	2-story		5-story		15-story	
	Plan-1	Plan-2	Plan-1	Plan-2	Plan-1	Plan-2
Cape Mendocino1	0.00004890	0.00005038	0.0006633	0.0007998	0.005445	0.005336
Cape Mendocino2	0.00005280	0.00005512	0.0008207	0.0006280	0.005576	0.007528
Northridge1	0.00005024	0.00005212	0.0007399	0.0009503	0.005648	0.005479
Northridge2	0.00005604	0.00005655	0.0005121	0.0005064	0.002001	0.002401
Northridge3	0.00004875	0.00005022	0.0005373	0.0005226	0.002097	0.002034
Landers	0.00005289	0.00005501	0.0005132	0.0004792	0.004213	0.003750
San Fernando	0.00004927	0.00005107	0.0010187	0.0013183	0.004518	0.004495
Average	0.00005127	0.00005292	0.00068645	0.0007435	0.004214	0.004432

of seven selected records. The selected accelerograms are scaled based on Iranian seismic code (2800 standard, which is similar to UBC 97) scaling method and then the maximum value of the displacements of roof mass center is obtained by applying the scaled accelerograms to the constructions. The mean value of the seven displacements obtained from this method is considered as the target displacement of the construction (Table 6). A good analogy for understanding accuracy and precision of ASCE/SEI 41-13 [32] coefficients method against the results of time history dynamic analysis has been achieved. The results of dynamic analyses confirmed the limit states declared by pushover analyses. The mean values obtained by dynamic analyses are greater than those of ASCE/SEI 41-13 [32] coefficients method except for 2-story buildings. The effects of higher modes and behavior change of taller RCTF constructions, which are not considered by pushover analyses as distinguished by Balkaya and Kalkan [2] may be considered for this observation.

7. Effect of wall percentage and eccentricity

With reference to Fig. 6, the impacts of changes of the wall percentage and the rate of eccentricity on the degree of building damage caused by earthquakes may be deduced. It should be noted that wall cross-section area percentage (wall percentage) in Y-direction and eccentricity perpendicular to Y-direction (e_x) in Plan-2 are 10.1% and 68.5% greater than the similar items in Plan-1, respectively. Comparative study of the diagrams of the 2-story constructions shows that construction Plan-2 has higher lateral strength, lower ductility and lower induced damage at all performance levels with respect to construction Plan-1.

The reasons of such behavior may be explained by comparing the wall percentages of the two plans. The lateral stiffness and strength of constructions increase when the shear wall ratio increases. However, the ductility is decreased for the same seismic intensity.

The destructive torsional effect caused by plan irregularity in a construction is usually aggravated by increasing construction height and

dominated by higher modes on its seismic behavior. In low-rise constructions, it does not have considerable negative impacts on construction behavior. Therefore, in spite of having a greater eccentricity, construction with Plan-2 incurs less damage as compared with Plan-1 pertaining to higher lateral stiffness/strength. In other words, greater wall percentage is a positive factor that can be able to reduce vulnerability induced by strong ground motions.

The torsional effects induced more destructive damage on taller buildings. For this reason, constructions with Plan-2 with greater eccentricity experience greater lateral strength degradation and failure than those with Plan-1. However, more wall percentage of Plan-2, as an effective factor in construction strength acts against the destructive effects of torsion, and hence compensates for the considerable amount of strength reduction, as long as damages are reduced. For this reason, the degree of damages induced on constructions with Plan-2 is relatively close to those of constructions with Plan-1. It can be concluded that the increase of wall percentage could somehow compensate the negative effects of more eccentricity value in the constructions up to an acceptable degree.

8. The multilevel definition of response modification factor (R-factor)

To the best of the authors' knowledge, there is not any seismic code or technical document to address the R-factor for irregular RCTF constructions so far. Due to application of this factor for code-based seismic design of this type of buildings, exploring R-factor seems more important to designers in urban areas where symmetrical construction is not possible. In design of structures against seismic loads, the ability of a structure to withstand earthquake forces through tolerating nonlinear deformation (induced damages) without a predefined damage (usually life safety limit state) is considered by means of reducing the elastic strength of structure by R-factor.

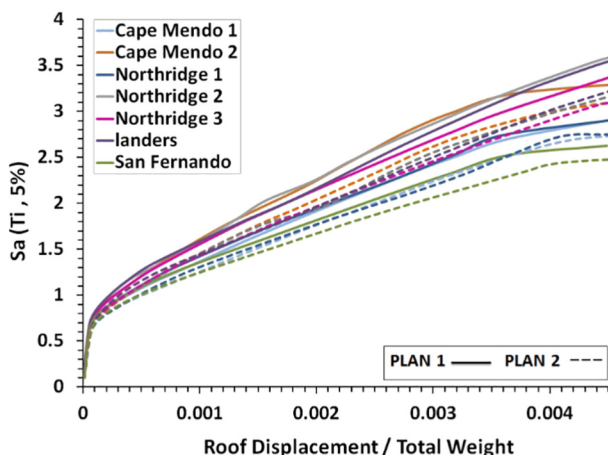


Fig. 11. IDA curves for the 2-story structure (Plan-1, 2).

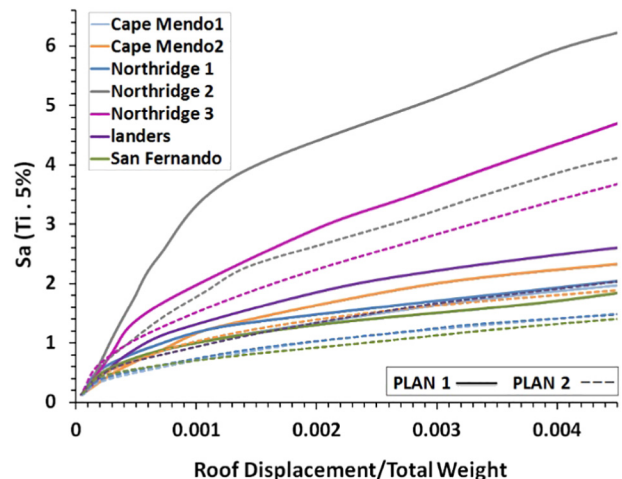


Fig. 12. IDA curves for the 5-story structure (Plan-1, 2).

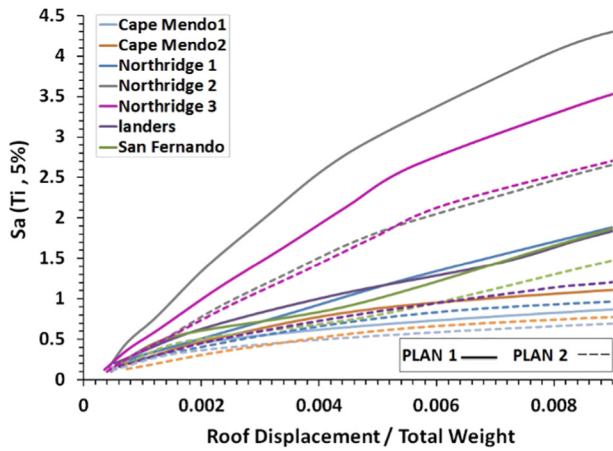


Fig. 13. IDA curves for the 15-story structure (Plan-1, 2).

Reviewing the methods for analytical estimation of this factor indicates that three distinct definitions may be identified. i) Code-based factor (force based). ii) Demand-based factor. iii) Supply-based factor [34–36]. Empirical R value in codes is based on tentative judgments and observing damages in past earthquakes and has been defined as the ratio of the actual to the design lateral strength. The concept of R in codes is considered based on the assumption that well-detailed seismic structural systems are able to undergo large inelastic deformations (life safety limit state) without sudden loss of their strength. The R values which are dedicated to all structures in design codes are more close to values determined by demand definition of R-factor.

In the technical literatures related to estimating behavior factors of structures, there are two distinct definitions for demand and supply R-factor. Using the behavior factor to convert elastic strength to yield strength in seismic codes specifies the damage accepted by codes. The degree of nonlinear deformations induced in structures subjected to earthquake depends upon ground motions intensity level and predefined performance level (acceptable damages). Predefining each of ground motion intensity level or performance level yields a different behavior factor as demand and supply R-factor.

Recently the Applied Technology Council developed a methodology to assess seismic design. This document contains a new methodology to quantify R-factor. The procedure commences through initial assumption of R-factor to design a series of archetype constructions. Then push-over and incremental dynamic analysis are applied to compute median collapse intensity. The Collapse Margin Ratio (CMR) is calculated as the ratio between the median collapse intensity and the Maximum Considered Earthquake (MCE) intensity. The three-dimensional effect of analytical modeling and earthquake excitation in addition to the spectral shape factors are considered to adjust CMR. The adjusted CMR (ACMR) is compared to accept ACMR for each archetype constructions. An iterative method is used by calculating the ACMRs to identify the

Table 7
The maximum base shear values considering elastic behavior of the structures.

Record	V _e (ton)					
	2-Story		5-story		15-story	
	Plan-1	Plan-2	Plan-1	Plan-2	Plan-1	Plan-2
Cape Mendocino1	195.74	204.84	702.36	659.12	1213.40	1137.32
Cape Mendocino2	205.25	206.04	991.74	808.27	2885.40	2592.16
Northridge1	198.29	205.06	793.56	687.65	3421.40	2690.93
Northridge2	207.00	226.73	860.15	997.07	1366.70	1188.71
Northridge3	194.77	210.50	803.12	816.70	1258.80	1203.59
Landers	212.68	220.43	841.51	651.22	2789.80	2535.47
San Fernando	203.44	211.23	827.01	673.88	1622.50	1490.55
Average	202.45	212.12	831.35	756.27	2079.71	1834.11

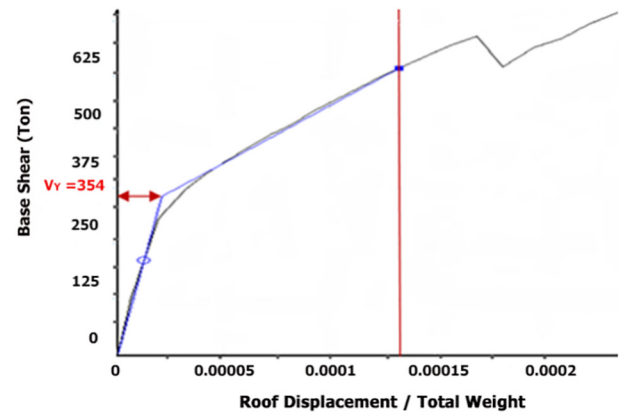


Fig. 14. An example of bi-linearization of the base shear-root displacement diagram of the 5-story structure (Plan-2).

failing or passing of the acceptance criteria for each archetype model (FEMA P695) [37]. The R-factor obtained from this method may be placed in demand based R-factor category. Although some advantages such as considering safe margin for collapse and rough incorporation of system collapse uncertainty can be devoted to this method, but explicit definition of R for various performance levels and seismic intensities are absent in this methodology.

In this section an explicit definition of performance based R-factor for both demand and supply category for RCTF buildings that has not yet been explored in the literatures, is introduced. The Incremental Dynamic Analysis (IDA) is used to determine demands and capacity of structures in multiple seismic intensities and limit states. IDA curve indicates the structure responses versus increasing intensity of a set of applied records. The selected parameters for intensity measure (IM) and damage measure (DM) should appropriately indicate the impact of an earthquake and behavior of a construction, respectively. Peak roof drift ratio among the common parameters is chosen for estimating DM. For IM parameter, spectral acceleration Sa(T1, 5%), at fundamental elastic natural period among other intensity measures is selected. In developing IDA curves, choosing suitable intensity scale is an important issue. It is preferred that the selected IM takes advantage of both efficiency and sufficiency. The efficiency is associated to minimize the scatter in the results requiring only a few ground motion records to provide good demand and capacity estimates. The sufficiency is attributed to provide a complete characterization of the response, without the need for magnitude or site-to-source distance information of suit of seismic records. It was indicated that both advantages of efficiency and sufficiency for S_a intensity measure were used versus peak roof drift ratio [38,39]. To develop all IDA curves, each pair of horizontal components of the earthquake record is applied simultaneously. The major component of the record that has usually the largest peak ground acceleration (PGA) is scaled to target intensity and then the same magnification

Table 8
The maximum base shear values considering non-linear behavior of the structures.

Record	V _y (ton)					
	2-Story		5-story		15-story	
	Plan-2	Plan-1	Plan-2	Plan-2	Plan-1	Plan-2
Cape Mendocino1	131.00	110.00	310.40	335.60	452.40	496.96
Cape Mendocino2	141.00	112.00	319.90	321.40	449.60	505.13
Northridge1	135.00	110.00	315.10	338.80	449.60	483.94
Northridge2	144.00	113.00	297.80	312.00	280.10	296.80
Northridge3	130.00	113.00	299.40	313.60	282.90	301.74
Landers	141.00	114.00	299.40	310.40	487.40	524.73
San Fernando	132.00	112.00	327.70	354.50	473.40	495.46
Average	136.29	112.00	309.96	326.61	410.77	443.54

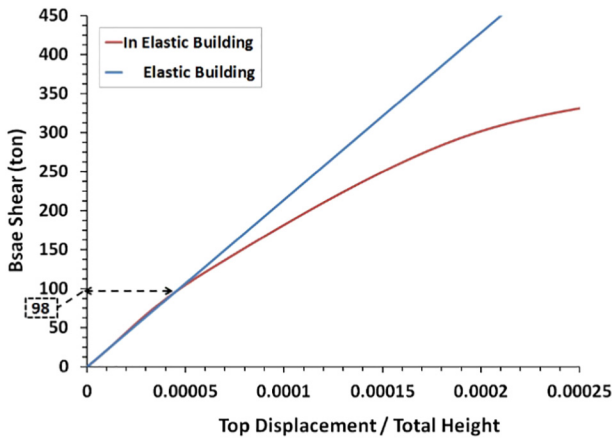


Fig. 15. An example of determination of V_s for the 5-story structure (Plan-2).

factor is applied to the minor component. So the relative intensities of the two components are maintained during increasing intensity.

The IDA curves obtained from multiple response history analysis are shown in Fig. 11-13.

8.1. The demand R-factor

Demand R-factor for MDOF systems can be determined through two methods. In the first one, demand R-factor is calculated for equivalent SDOF system and then this factor is corrected for the MDOF system. In the second way, it is possible to obtain R-factor directly from MDOF construction [40]. Here, the second method is applied.

The demand R-factor can directly be calculated for a MDOF construction as:

$$R_{Demand}^{MDOF} = R_{\mu}^{MDOF} \cdot \Omega_d \cdot R_d \tag{8}$$

Where;

R_{μ}^{MDOF} = ductility reduction factor for MDOF systems and taking into account the dissipated energy caused by nonlinear behavior.

Ω_d = factor for regarding the redundancy and redistribution of internal forces.

R_d = modification factor for code based design.

Since the demand R-factor of a structure depends on the level of regional seismic hazard of a site (intensity of ground motion), the first step is to select the records consistent with the seismic hazard level of

the site. To achieve such an objective, seven accelerograms of Table 5 are selected and scaled to the design acceleration spectrum of Iranian seismic code for high level of seismic hazard [24].

To estimate ductility reduction factor of a MDOF construction, dynamic analyses are performed by applying scaled accelerograms in two stages. At first stage by assuming linear behavior, the mean of the maximum base shears obtained by the first analyses is considered as V_e (Table 7). Then to estimate V_y , the maximum values of roof drift for each of the seven performed non-linear analyses of the constructions are extracted. Then, yield shear strengths for maximum roof drift through bi-linearization of the pushover curve based on ASCE/SEI 41-13 [32] rule are obtained (Fig. 14). Mean of the seven base shears achieved from this method is considered as V_y (Table 8).

The ductility reduction factor is evaluated from following relationship.

$$R_{\mu}^{MDOF} = \frac{V_e}{V_y} \tag{9}$$

The over-strength modification factor is obtained from the ratio of yield strength to the strength corresponding to formation of the first plastic hinge in the construction (Eq. (10)). Regarding Fig. 15, V_s value (first-local yield strength) can be considered equal to the first separation point of the base shear-roof displacement of nonlinear construction from a line corresponding to elastic stiffness (evaluated and depicted in Fig. 16).

$$\Omega_d = \frac{V_y}{V_s} \tag{10}$$

In allowable stress/ultimate strength design, values of strengths of materials/loads are multiplied by reduction/magnification factors in design process. To reduce first-local yield strength to design strength (V_{design}), R_d factor is used (Eq. (11)). V_{design} is calculated as $V_{design} = W.S_a/R$ in which, R is presumed as the modification factor (or predefined R-factor). Here the presumed R of 5.5 is considered for constructions (Fig. 16).

$$R_d = \frac{V_s}{V_{design}} \tag{11}$$

Finally, the R-Demands are estimated based on Eq. (8), which are depicted in Fig. 17.

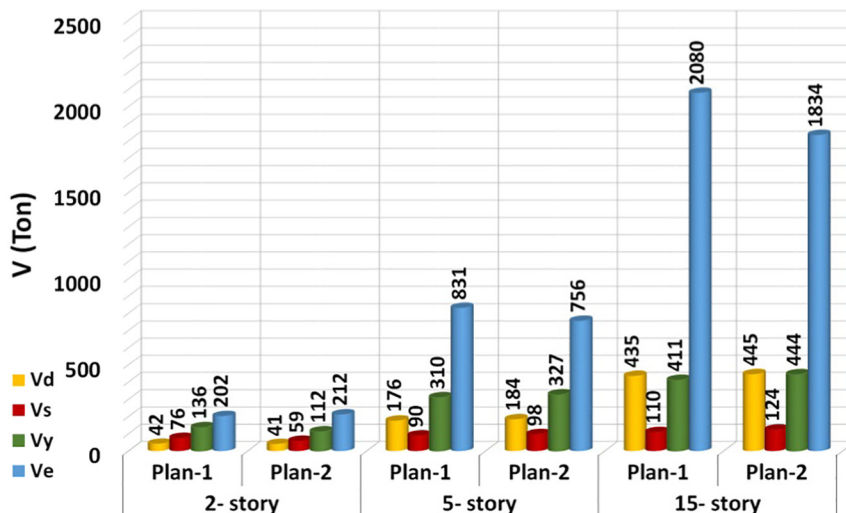


Fig. 16. V_d , V_s , V_y , and V_e values for the under study structures.

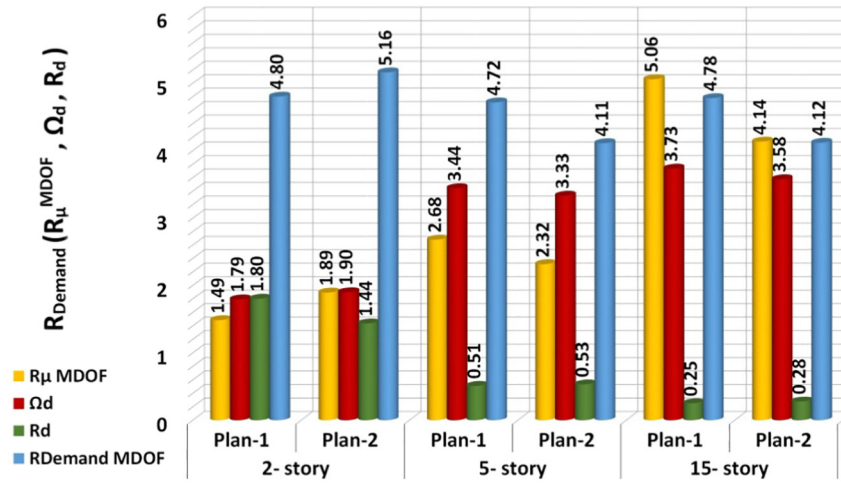


Fig. 17. R_{Demand} values for the under study structures.

8.2. The supply R-factor

R_{Supply} may be defined at each performance level. It requires determining construction capacity at different predefined acceptable damage levels. Thus, optimistically in the case of designing the new construction through force method and using this R-factor, the designed construction subjected to an earthquake with the specified intensity, is capable of satisfying the relevant performance levels. The performance levels can be expected relating to the acceptable damage level, the construction system type, and its degree of importance. The damages induced by earthquake associated to each performance level can be defined as local and global seismic damages.

To estimate supply R-factor in this study, the same selected seven accelerograms applied for calculating demand R-factor are used. The damages induced at spandrels are considered as local damages and the ones associated to walls are considered as global damages. The steps to calculate R_{Supply} are similar to that of R_{Demand} calculation. The only difference is that R should be determined at relevant performance level.

In summary, R_{Supply} has been estimated through the following steps:

- The construction is analyzed by non-linear static analysis subjected to triangular lateral loading pattern and then displacement of the roof mass center corresponding to every performance level is determined (Table 3).
- IDA curves are developed through applying the seven selected accelerograms and then intensity values (S_a) corresponding to each failure level are determined based on the roof drift ratio.
- The seven selected accelerograms scaled to previous step intensity values (S_a) corresponding to each failure level are imposed to the

construction assuming elastic behavior. The maximum value of base shear for each analysis is recorded and their mean value is considered as V_e (Fig. 18).

- The base shear of yield strength (V_y) can be estimated through bi-linearization of the base shear-roof drift ratio diagram obtained from non-linear static analysis of construction at target displacement corresponding to each performance level (Fig. 18). The ductility reduction factor is evaluated from Eq. (9).
- The base shear corresponding to the formation of the first plastic hinge of construction (V_s) based on procedure explained in R_{Demand} is determined. The over-strength modification factor (Ω_s) is obtained from Eq. (10).
- There is no difference between R_d values in determining R_{Demand} and R_{Supply}
- The R_{Supply} are estimated based on Eq. (12) and they are depicted in Fig. 19 for all case study constructions.

$$R_{Supply}^{MDOF} = R_{\mu}^{MDOF} \cdot \Omega_s \cdot R_d \tag{12}$$

Since bringing a construction to each damage level (performance level) depends on intensity of input excitations, it is possible to present values of supply R-factor (R_{Supply}) in terms of both intensity measure and predefined damage level in the form of performance-based classification for the under studied structures, which are depicted in Fig. 20. PGA_i values, in each case, indicate maximum intensity measure of input excitation that the construction is still at the specified performance level. In this study, PGA_i is obtained from mean of maximum

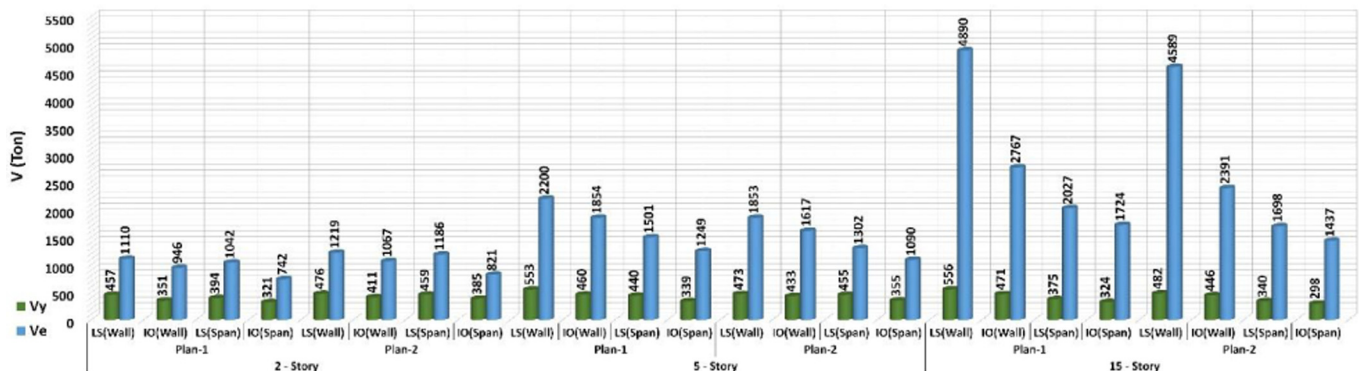


Fig. 18. V_y, V_e values for the under study structures.

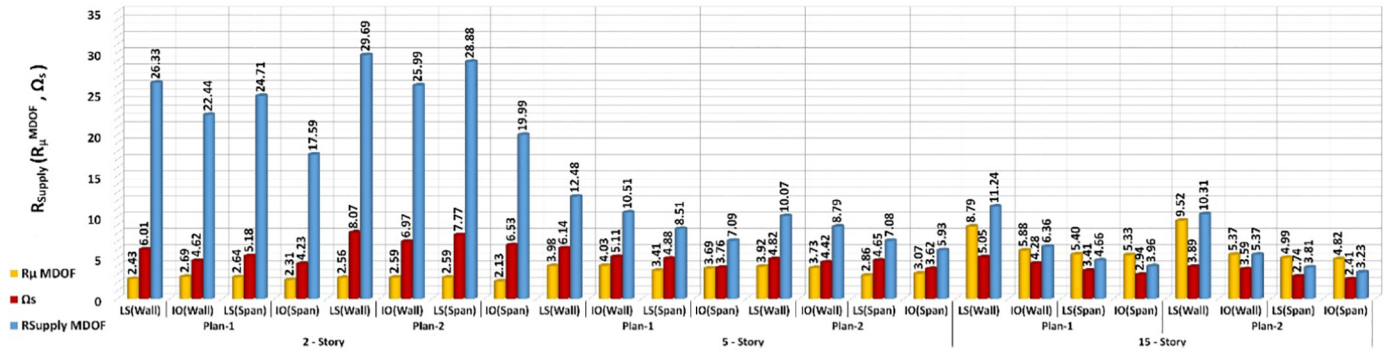


Fig. 19. R_{Supply} values for the under studied structures.

PGA related to each applied record that the construction is still at the relevant performance level.

9. Conclusions

In analytical framework for the results obtained by this study the following conclusions have been drawn.

1. The results of this study indicate that contrary to the concerns regarding the weak performance of this structural system against seismic torsional response, its high lateral stiffness and strength compensates its low initial torsional stiffness. It has also met the seismic design requirements in spite of the irregularity.
2. Since diagonal reinforcements required for shear strength are not practically possible to implement, the spandrels will fail at the onset of entering structural system into nonlinear range of deformations. For low-rise constructions (under 5 stories), due to lack of incorporating spandrels in lateral strength of construction, using these low shear strength spandrels cannot cause substantial damage. For taller ones with additional membrane elongation pertaining to larger shear distortion demand, such spandrels would be collapsed much sooner than shear walls. Therefore, these elements do not have significant effect on final failure strength of a construction, but in turn, cause a small and temporary increase of its lateral strength.

Therefore, for high-rise construction the special design of spandrels as the seismic energy dissipating device is recommended.

3. R_{Supply} is much larger than R_{Demand} for 2- and 5-story structures at all performance levels. This is an indication of the high capacity of these structures in spite of their irregularities. The comparison of the parameters involved in R_{Supply} shows that the Ω_s values of 2- and 5-story structures are much larger than those of other involved parameters at all performance levels that indicates high redundancy of this box-type of structural system.
4. R_{Supply} is smaller than R_{Demand} only for the 15-story structure at all performance levels for spandrels. As explained in item 2, considering the fact that the existing low shear strength spandrels do not affect generally the seismic performance of the structure it is even recommended that they should not be used in analytical modeling of RCTF structure as the primary structural elements. R_{Supply} values for the 15-story structure are also larger than its R_{Demand} values by setting R_{Supply} at the performance levels for shear walls as the criterion.
- i. The R values calculated in this research are obtained from investigating only 5 irregular RCTF structures. Most certainly, with the limited scope of this study, these R-factor values are valid for understudied structures. Considering the importance of R-factor in code-based design of structures determines that R-factor of irregular tunnel form structures requires extensive research work pertaining to different

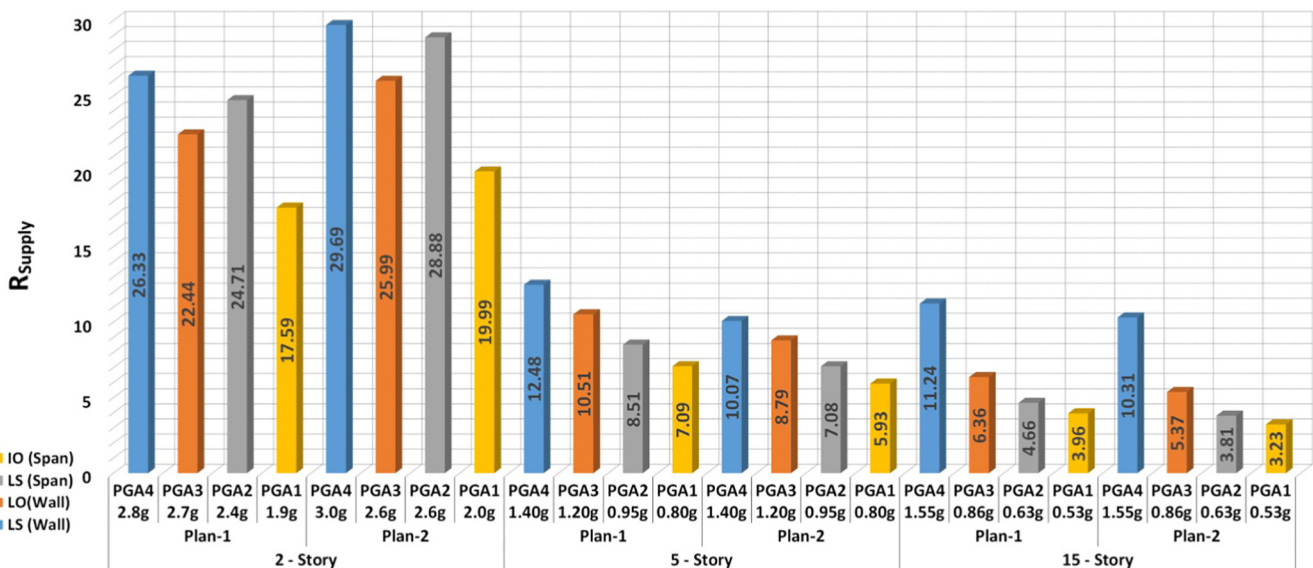


Fig. 20. Performance-based classification for R_{Supply} of the under study structures.

levels of eccentricity, and heights. Hopefully, researchers will take effective steps towards this topic in future.

References

- [1] Sotoudeh Y, Salehi M, Moradzadeh S, Taghipoor H, Behboodi M. Building technology for mass concrete tunnel form method. *Advances in Environmental Biology* 2013; 7(9):2190–4 [ISSN 1995–0756].
- [2] Balkaya C, Kalkan E. Nonlinear seismic response evaluation of tunnel form building structures. *Computers and Structures* 2003;81:153–65.
- [3] Kalkan E, Yuksel SB. Pros and cons of multistory RC tunnel-form (box-type) buildings. *Struct Design Tall Spec Build* 2007;17:601–17. <http://dx.doi.org/10.1002/tal.368>.
- [4] Goel RK, Chopra AK. Period formulas for concrete shear wall building. *Journal of Structural Engineering* 1998;124(4):426–33.
- [5] NEHRP1994. Recommended Provisions for the Development of Seismic Regulations for New Buildings. Washington, D.C.: Building Seismic Safety Council; 1994
- [6] SEAOC-96. Recommended Lateral Force Requirements and Commentary. Seismology Committee, Structural Engineers Association of California; 1996.
- [7] UBC-97 Uniform Building Code. Int. Conf. of Building Officials, Whittier, California; 1997.
- [8] Lee L, Chang K, Chun Y. Experimental formula for the fundamental period of RC buildings with shear wall dominated systems. *Structural Design of Tall Buildings* 2000;9(4):295–307.
- [9] KBC1998. National Building Code of Korea. The Ministry of Construction; 1988.
- [10] NBCC National Building Code of Canada. Associate Committee on the National Building Code, National Research Council of Canada, Ottawa 1995 NRCC 23174; 1995[454 p].
- [11] BSLJ 1994 Building Standard Law of Japan. Building Center of Japan; 1994.
- [12] Balkaya C, Kalkan E. Estimation of fundamental periods of shear-wall dominant building structures. *Earthquake Engineering and Structural Dynamics* 2003;32(7): 985–98. <http://dx.doi.org/10.1002/eqe.258>.
- [13] Balkaya C, Kalkan E. Relevance of r-factor and fundamental period for seismic design tunnel form buildings. 13th World Conference on Earthquake Engineering Vancouver 2004; [Paper no: 3153]. Vancouver, B.C., Canada
- [14] Eshghi S, and Tavaafoghi A. Seismic behaviour of tunnel form concrete building structures. The 14th World Conference on Earthquake Engineering 2008; Beijing, China
- [15] ASCE/SEI 7-05. Minimum design loads for buildings and other structures. 1801 Alexander Bell Drive, Reston, Virginia 20191; American Society of Civil Engineers; 2006.
- [16] Eshghi S, Tavaafoghi A. Seismic behaviour of tunnel form building structures: an experimental study 2012 [15WCEE].
- [17] Balkaya C, Kalkan E. Seismic vulnerability, behavior and design of tunnel form buildings. *Eng Struct* 2004;26(14):2081–99. <http://dx.doi.org/10.1016/j.engstruct.2004.07.005>.
- [18] Tavaafoghi A, Eshghi S. Evaluation of behavior factor of tunnel-form concrete building structures using applied technology Council 63 methodology. *Struct Design Tall Spec Build* 2013;22(8):615–34.
- [19] ACI 318-05. Building Code Requirements for Structural Concrete and Commentary. Reported by ACI committee; 2004.
- [20] BHRC-Building and Housing Research Center of Iran, Office for Developing and Promoting National Building Codes. Design and Construction of Reinforced Concrete Buildings; 2006.
- [21] Ministry of Public Works and Housing. Regulation for Buildings in Seismic Areas. Official Gazette; 2007.
- [22] O'zuygur AR. Performance-based seismic design of an irregular tall building – a case study. *Journal of Structures* 2016;5:112–22 [The Institution of Structural Engineers] <http://dx.doi.org/10.1016/j.istruc.2015.10.001>.
- [23] INBC. Iranian National Building Code for Loading Part 63rd ed. ; 2014.
- [24] Standard 2800. The Code for Designing Buildings Against Earthquakes. 3rd ed. Tehran: Housing Research Center Publications; 2013.
- [25] CSI. Perform-3D, Version4. Nonlinear Analysis and Performance Assessment for 3D Structures. Berkeley, California 94704 USA: Computer and Structures INC; 2006.
- [26] Mander JB, Priestley MJN, Park R. Observed stress-strain behavior of confined concrete. *Journal of Structural Engineering* 1988;114(8):1827–49.
- [27] Mander JB, Priestley MJN, Park R. Theoretical stress-strain model for confined concrete. *Journal of the Structural Division* 1988;114(8):1804–26.
- [28] Esmaily A, Xiao Y. Behavior of reinforced concrete columns under variable axial loads. *ACI Structural Journal* 2005;101(1):124–32.
- [29] Napier J. Modeling of coupling beams in shear walls. In: Powell GH, editor. Technical Note. Berkeley: UC; 2013 Edited by <https://wiki.csiamerica.com>.
- [30] Yuksel SB, Kalkan E. Behavior of tunnel form buildings under quasi-static cyclic lateral loading. *Structural Engineering and Mechanics* 2007;27(1).
- [31] Harries KA, Gong B, Shahrooz BM. Behavior and design of reinforced concrete, steel, and steel-concrete coupling beams. *Earthq Spectra* 2000;16(4):775–99. <http://dx.doi.org/10.1193/1.1586139>.
- [32] ASCE/SEI 41-13. Seismic Evaluation and Retrofit of Existing Buildings. American Society of Civil Engineers; 2014. <http://dx.doi.org/10.1061/9780784412855>.
- [33] Mosleh A, Rodrigues H, Varum H, Costa A, Arêde A. Seismic behavior of RC building structures designed according to current codes. *Journal of Structures* 2016;7:1–13 [The Institution of Structural Engineers] <http://dx.doi.org/10.1016/j.istruc.2016.04.001>.
- [34] Uang CM. Establishing R (or R_w) and Cd factors for building seismic provisions. *Journal of Structural Engineering* 1991;117(1):19–28.
- [35] Miranda E, Bertero V. Evaluation of strength reduction factors for earthquake-resistant design. *Earthquake Spectra* 1994;10(2):357–79. <http://dx.doi.org/10.1193/1.1585778>.
- [36] ATC-19. Structural Response Modification Factors. Redwood City, California: Applied Technology Council; 1995 5–32.
- [37] FEMA P695. Quantification of Building Seismic Performance Factors. Washington, DC, USA: Federal Emergency Management Agency; 2009.
- [38] Vamvatsikos D. Seismic Performance Capacity and Reliability of Structures as Seen Through Incremental Dynamic Analysis. [PhD thesis] Stanford University; 2002.
- [39] Zameeruddin M, Sangle KK. Review on Recent developments in the performance-based seismic design of reinforced concrete structures. *Journal of Structures* 2016; 119–33 [The Institution of Structural Engineers] <http://dx.doi.org/10.1016/j.istruc.2016.03.001>.
- [40] Mwafy AM, Elnashai AS. Calibration of force reduction factors of RC buildings. *Journal of Earthquake Engineering* 2002;6(2):239–73. <http://dx.doi.org/10.1142/S1363246902000723>.